Path Tracking Error Analysis for Underwater Glider Navigation in a Spatially and Temporally Varying Flow Field

Mengxue Hou, Shijie Liu, Fumin Zhang, Catherine R. Edwards

***Abstract*—In this paper, we presented path tracking error comparison between two navigation schemes for underwater glider that combine path planning and a path tracking controller. Path planning is performed with the time-averaged flow field for both schemes, while path tracking is performed with the instantaneous or the time-averaged flow field. Mathematical analysis and numerical simulation show that performing path tracking control with instantaneous flow results in smaller path tracking error when the strength of spatially varying flow is small compared to glider speed, while it leads to larger path tracking error if spatially varying flow is the same order as the glider speed. Performing path tracking control with instantaneous flow leads to less path tracking error when the spatially varying flow is of relatively high frequency, but it produces larger path tracking error if the spatially varying flow is of low frequency. Simulated experiments near Cape Hatteras, NC show that in this specific region, performing path tracking control with instantaneous flow results in less path tracking error, which is consistent with the analytical result.**

I. Introduction

Underwater gliders are moving robotic sensing platforms [1] that are able to perform persistent surveying missions in the ocean for data collection [2]–[4]. They take advantage of buoyancy and attitude to move through the water column [5]–[8], surfacing at defined intervals to communicate with the onshore dockserver to receive mission updates and commands.

Control and navigation of underwater gliders can be achieved through a combined path planning and path tracking control scheme. Path planning designs an optimal path connecting the glider's current position with the destination position. Then, a path tracking controller computes a series of steering angle that drives the glider to follow the designed optimal path. Flow canceling strategy was introduced in [9] to track, or follow, the path. It computes the steering angle to cancel the flow component orthogonal to the heading direction, such that at each timestep, the addition of glider speed and flow velocity coincides with the predefined heading direction.

In order to perform this glider control scheme, flow prediction of high accuracy and resolution is a necessity. The path planning algorithm requires flow prediction data from the present time to the time when glider reaches the destination (usually at the timescale of days or weeks), while the path tracking controller requires a prediction of flow over just one diving/surfacing interval (usually 3-6 hours). Operationally, a 12-24 hour prediction provides a failsafe should the glider miss a surfacing. Operational ocean models typically publish 24-96 hour forecasts, with model error increasing with the length of the forward prediction, due to missing physics in a model, errors in the model forcing terms and boundary conditions [10], [11]. In our previous paper [12], we proposed using the time-averaged temporally-invariant flow map as input to the path planning algorithm, and then used either the time-averaged or instantaneous flow map as input to the path tracking controller. Assuming that the instantaneous flow field consists of only temporal variability, a comparison on path tracking error and travel time of the two control schemes was presented.

In this paper, we will further extend our prior discussion [12]. Instead of considering only the temporal variability as in the previous work, we provide path tracking error comparison results in a flow field containing both spatial and temporal variability. Assuming that the flow field can be modeled by the sum of a spatially varying flow component and a temporally varying flow component, the goal of this paper is to compare the path tracking error of using the instantaneous flow and the time-averaged flow field for path tracking controller. Both the spatial and temporal variability of the flow field are modeled by sinusoidal function, chosen to represent tidal variability in time and a generalized scale for spatial variability. The cross-track path tracking error dynamics is analyzed, and the path tracking error of using the two control schemes is computed and compared numerically in different flow conditions.

The novelty of this paper lies in that we provide a method to select a controller that reduces path tracking error in the case where the flow prediction input to path planning controller is unavailable. Previous work has analyzed the evolution of path tracking error given a biased flow map [13], [14], but in this study, no specific flow map prediction is assumed to be known, except for the periodic feature of the flow field. This proposed scheme would be helpful to the study of control and navigation of underwater gliders in the case where no accurate flow prediction is available.

The rest of the paper is organized as follows. The problem is formulated in Section II. The analysis and numerical simulation on path tracking error comparison of the two

Mengxue Hou and Fumin Zhang are with the School of Electrical and Computer Engineering, Georgia Institute of Technology, Atlanta, Georgia 30308, {mhou30, fumin}@gatech.edu

Shijie Liu is with Shenyang Institute of Automation, Chinese Academy of Sciences, China 110016. liushijie@sia.cn

Catherine R. Edwards is with Skidaway Institute of Oceanography, Department of Marine Science, University of Georgia, Savannah, Georgia 31411. catherine.edwards@skio.uga.edu

978-1-5386-4814-8/18/$31.00 ©2018 IEEE

control schemes are presented in Section III. In Section IV, a simulation example of glider path tracking error comparison using the two control scheme is shown. Finally, Section V presents the conclusions based on the results of mathematical analysis and simulated experiment.

II. Problem Formulation

In this work, we consider a slow-moving underwater glider traveling over a large temporal and spatial scale. Therefore, details of the vehicle kinematics can be ignored, and a simple kinematic model is used to represent glider dynamics:

$$\dot{\mathbf{x}} = \mathbf{F}(\mathbf{x}, t) + \mathbf{u}(\mathbf{x}, t), \tag{1}$$

where the state $\mathbf{x}(t) = [x_1(t), x_2(t)]^T \in \mathbb{R}^2$ represents glider horizontal position. $\mathbf{F} : \mathbb{R}^2 \times [t_0, t_1] \to \mathbb{R}^2$ denotes a temporally and spatially varying flow field, and $\mathbf{u}(\mathbf{x}, t)$ describes glider through-water velocity.

The goal of this paper is that, given a feasible and time-optimal path planned in the time-averaged flow field, we can select a path tracking controller between two candidates to drive a glider through a spatially and temporally varying flow field to follow the designed path and reach the goal point with reduced path tracking error compared to the other one.

A. Path planning and path tracking strategy

We denote the planned path as $\{\mathbf{z}_i\}_{i\in\{1,2,...,P\}} \in \mathbb{R}^2$, and assume that the planned path is feasible for a glider to travel on in the time-averaged flow field. A path is defined as feasible if at each timestep, there exists a steering angle that can drive the glider to go from the current position on the path, $\mathbf{z}_i, i \in 1, 2, ..., P-1$, to reach the next position, $\mathbf{z}_{i+1}$ in finite time.

In this work, the path planning algorithm is performed with the time-averaged flow field. Since in the experiments, the lunar semidiurnal M_2 tide is significant, averaging is taken over two times the M_2 period (12.42 hours). The time averaged flow field is denoted as $\bar{\mathbf{F}}(\mathbf{x}, t)$.

The flow canceling strategy is used to design the glider steering angle to follow a series of heading directions under the influence of flow. Here the series of heading directions is given by the planned path. Let $\mathbf{T}$ be a unit vector describing the heading direction, then it can be described by the tangent direction of the planned path. The cross-track direction is defined as $\mathbf{N} = \mathbf{J}\mathbf{T}$, where $\mathbf{J}$ is the 90° rotation matrix.

The flow canceling strategy chooses a glider steering angle by trying to cancel the cross-track flow to maintain the heading angle. However, if the cross-track flow speed is larger than the glider speed at certain time and position, then glider speed will be assigned to cancel the cross-track flow, in order to minimize its deviation in directed heading. Considering the above two cases, the flow canceling strategy can be written as the following equations:

$$\begin{aligned} \mathbf{u}(\mathbf{x}, t)^T\mathbf{T} &= \sqrt{\alpha^2 - (sat_\alpha(\mathbf{F}(\mathbf{x}, t)^T\mathbf{N}))^2}, \\ \mathbf{u}(\mathbf{x}, t)^T\mathbf{N} &= -sat_\alpha(\mathbf{F}(\mathbf{x}, t)^T\mathbf{N}), \end{aligned} \tag{2}$$

where α denotes glider through water speed, $sat_c(\cdot)$ denotes a saturation function $sat_c : \mathbb{R} \to [-c, c]$.

B. Path tracking error

We consider a simulated virtual glider with initial position same as the real glider, and is also navigated by flow canceling strategy to follow the planned path. We assume that the simulated glider is moving in the time-averaged flow field $\bar{\mathbf{F}} : \mathbb{R}^2 \times [t_0, t_1] \to \mathbb{R}^2$. The dynamics for the simulated glider is described as

$$\dot{\mathbf{z}} = \bar{\mathbf{F}}(\mathbf{z}, t) + \mathbf{u}(\mathbf{z}, t), \tag{3}$$

where $\mathbf{z} \in \mathbb{R}^2$ denotes horizontal position of the simulated glider. Path tracking error $\mathbf{e}(t)^T\mathbf{N}$ is defined as the difference between glider position $\mathbf{x}(t)$ and simulated glider position $\mathbf{z}(t)$ projected onto the cross-track direction. Thus the error dynamics can be described as follows:

$$\dot{\mathbf{e}}(t)^T\mathbf{N} = (\mathbf{F}(\mathbf{x}, t) + \mathbf{u}(\mathbf{x}, t) - \bar{\mathbf{F}}(\mathbf{z}, t) - \mathbf{u}(\mathbf{z}, t))^T\mathbf{N}, \tag{4}$$

with initial condition $\mathbf{e}(0)^T\mathbf{N} = 0$.

Note that since the path planning method guarantees to generate feasible path, the glider speed is able to completely cancel the time-averaged flow speed in the cross-track direction, $\bar{\mathbf{F}}(\mathbf{z}, t) + \mathbf{u}(\mathbf{z}, t) = 0$. Thus, the path tracking error dynamics in (4) can be simplified as

$$\dot{\mathbf{e}}(t)^T\mathbf{N} = (\mathbf{F}(\mathbf{x}, t) + \mathbf{u}(\mathbf{x}, t))^T\mathbf{N}. \tag{5}$$

III. Path Tracking Error Estimation

In this section, we will derive path tracking error of using instantaneous flow and time-averaged flow as input to flow canceling controller. We denote the starting and goal position as $\mathbf{r_s} = [x_{s1}, x_{s2}]^T, \mathbf{r_d} = [x_{d1}, x_{d2}]^T$, respectively. In order to simplify the analysis, we assume that $x_{s1} = x_{d1}, x_{s2} < x_{d2}$.

The flow field $\mathbf{F}(\mathbf{x}, t)$ is represented by the sum of a spatially varying function and a temporally varying function. We use $\bar{\mathbf{F}}(\mathbf{x}) = [a_r \cos\omega_r x_1, 0]^T$ to model the spatially varying flow component; the wavelength $\frac{2\pi}{\omega_r}$ represents a characteristic scale of spatial variability. The temporal variability of the ocean flow is modeled as a sinusoidal function with the M_2 period, $\mathbf{F}_t(t) = [a_t \cos\omega_t t, 0]^T$.

Since path planning is performed with the time-averaged flow field $\bar{\mathbf{F}}(\mathbf{x})$, the time-optimal path in this flow field is a straight line connecting the starting position with the goal position [15]. The along-track direction is $\mathbf{T} = [0, 1]^T$, and the cross-track direction is $\mathbf{N} = [1, 0]^T$. The along-track flow speed is 0 along the planned path, and the cross-track flow speed at glider position $\mathbf{x}$ at time t can be described as

$$\begin{aligned} \mathbf{F}(\mathbf{x}, t)^T\mathbf{N} &= (\bar{\mathbf{F}}(\mathbf{x}) + \mathbf{F}_t(t))^T\mathbf{N} \\ &= a_r \cos\omega_r x_1(t) + a_t \cos\omega_0 t. \end{aligned} \tag{6}$$

Let us consider the path tracking error in the following two cases of performing path tracking control with the instantaneous flow and time-averaged flow. For each of the cases, two sub-cases are considered.

A. Case 1: Performing path tracking control with instantaneous flow field

In this case, according to (2), the glider's cross-track through-water speed can be described as

$$\mathbf{u}(\mathbf{x},t)^T\mathbf{N} = \begin{cases} -\alpha & \text{if } a_r\cos\omega_r x_1 + a_t\cos\omega_t t > \alpha \\ \alpha & \text{if } a_r\cos\omega_r x_1 + a_t\cos\omega_t t < -\alpha \\ -a_r\cos\omega_r x_1 & \\ -a_t\cos\omega_t t & \text{otherwise} \end{cases}. \quad (7)$$

Let us compute the path tracking error in the following two flow sub-cases.

a) Glider speed always larger than instantaneous flow speed. In this case, $a_r + a_t \leq \alpha$. Thus the glider's speed is always able to cancel the instantaneous cross-track flow speed that glider experiences along its trajectory. Therefore, path tracking error is always zero along the trajectory.

b) The instantaneous flow speed is comparable to glider speed. In this case, $a_r \leq \alpha \leq a_r + a_t$. With the glider cross-track through water speed described in (7), and the path tracking error dynamics represented by (5), the path tracking error growth follows

$$\dot{\mathbf{e}}(t)^T\mathbf{N} = \begin{cases} a_r\cos\omega_r x_1 & \\ +a_t\cos\omega_t t - \alpha & \text{if } a_r\cos\omega_r x_1 + a_t\cos\omega_t t > \alpha \\ a_r\cos\omega_r x_1 & \\ +a_t\cos\omega_t t + \alpha & \text{if } a_r\cos\omega_r x_1 + a_t\cos\omega_t t < -\alpha \\ 0 & \text{otherwise} \end{cases}. \quad (8)$$

In this case, it is difficult to compute $\mathbf{e}(t)^T\mathbf{N}$ by integrating its derivative. Instead, we will use numerical simulation to compute $\mathbf{e}(t)^T\mathbf{N}$, and compare with Case 2 in III-C.

B. Case 2: Performing path tracking control with time-averaged flow field

In this case, according to (2), the glider's cross-track through-water speed can be described as

$$\mathbf{u}(\mathbf{x},t)^T\mathbf{N} = \begin{cases} -\alpha & \text{if } a_r\cos\omega_r x_1 > \alpha \\ -a_r\cos\omega_r x_1 & \text{if } -\alpha < a_r\cos\omega_r x_1 \leq \alpha \\ \alpha & \text{if } a_r\cos\omega_r x_1 \leq -\alpha \end{cases}. \quad (9)$$

Similarly, let us look at the following two flow field sub-cases in order to compute the path tracking error.

a) Glider speed always larger than instantaneous flow speed. In this case, glider speed is always able to cancel the cross-track time-averaged flow speed along its trajectory. In this case, $a_r + a_t \leq \alpha$. According to the through-water glider speed described in (9) and the error dynamics represented by (5), the path tracking error dynamics in this sub-case is

$$\dot{\mathbf{e}}(t)^T\mathbf{N} = a_t\cos\omega_t t. \quad (10)$$

Then the path tracking error can be computed by integration:

$$\mathbf{e}(t)^T\mathbf{N} = \frac{a_t}{\omega_t}\sin\omega_t t. \quad (11)$$

Therefore in this case the path tracking error is bounded by $\frac{a_t}{\omega_t}$.

b) The instantaneous flow speed is comparable to glider speed. In this case, $a_r \leq \alpha \leq a_r + a_t$. With (9)and (5), the path tracking error dynamics in this sub-case can be derived as

$$\dot{\mathbf{e}}(t)^T\mathbf{N} = \begin{cases} a_r\cos\omega_r x_1 + a_t\cos\omega_t t - \alpha & \text{if } a_r\cos\omega_r x_1 > \alpha \\ a_r\cos\omega_r x_1 + a_t\cos\omega_t t + \alpha & \text{if } a_r\cos\omega_r x_1 < -\alpha \\ a_t\cos\omega_t t & \text{otherwise} \end{cases}. \quad (12)$$

Due to the difficulty of computing $\mathbf{e}(t)^T\mathbf{N}$ from its derivative, we will use numerical simulation to compute the path tracking error in III-C.

C. Path tracking error comparison

This part of the section will compare path tracking error of using path tracking controller with instantaneous flow and time-averaged flow field.

a) Glider speed always larger than instantaneous flow speed. In this case, performing flow canceling algorithm with the instantaneous flow field results in zero path tracking error, while performing flow canceling algorithm with the time-averaged flow field results in path tracking error bounded by $\frac{a_t}{\omega_t}$. Therefore, path tracking error is bounded if either instantaneous flow field or time-averaged flow field is the input for path tracking controller, but is minimized when using instantaneous flow for path tracking control.

b) The instantaneous flow speed is comparable to glider speed. In this case, we will compare path tracking error of using the two flow maps for path tracking controller by numerical simulation. Specifically, we will study how the path tracking error changes with respect to different $\frac{a_r}{\alpha}$, $\frac{a_t}{\alpha}$ and ω_r, and then determine if using the two control schemes result in bounded path tracking error. Note that we let $\omega_t = \frac{2\pi}{12.42*3600}(rad/s)$ to represent the M_2 tidal component.

First let us consider how path tracking error is affected by the strength of spatially and temporally varying flow components relative to vehicle speed. Denote the amplitude of spatially varying flow component normalized by glider's speed as $\rho = \frac{a_r}{\alpha}$, and the amplitude of temporally varying flow component normalized by glider's speed as $\gamma = \frac{a_t}{\alpha}, \rho, \gamma \in [0,1]$. Fig. 1 shows how the path tracking error varies for different ρ and γ values under the two control schemes, with $\omega_r = \frac{2\pi}{10^4}(rad/m)$ to represent a 10 km wavelength. In this figure, each grid cell in the domain represents a combination of ρ and γ; color of each cell describes the maximum absolute path tracking error along glider trajectory under this flow setting. Fig. 1a shows that path tracking error always stays zero if $\frac{a_t}{\alpha} + \frac{a_r}{\alpha} \leq 1$ under the first control scheme. This is consistent with the result presented in Sub-case 1 of III-A. The path tracking error becomes larger than zero as $\rho+\gamma$ gets larger than one. It reaches its maximum when $\rho = \gamma = 1$. Similarly, Fig. 1b describes path tracking error growth when path tracking is performed with time-averaged flow map. In this case, the bound of path tracking error is only changing

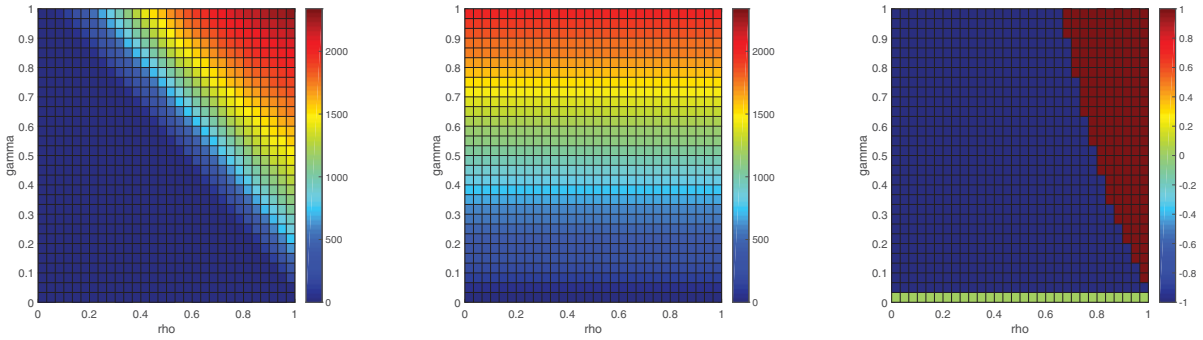

(a) Case 1. Path tracking error of performing flow canceling strategy with instantaneous flow field in 24 hours. Path tracking error unit is meter.

(b) Case 2. Path tracking error of performing flow canceling strategy with time averaged flow field. Path tracking error unit is meter.

(c) Sign of the difference between path tracking error of using instantaneous flow for path tracking controller and using time-averaged flow for path tracking controller.

Fig. 1: Numerical simulation showing how path tracking error changes with respect to ρ and γ. ρ and γ represent the strength of spatially and temporally varying flow components normalized by glider speed.

with γ, but is not changing with respect to ρ. This result is also consistent with the discussion in Sub-case 1 of III-B.

Fig. 1c shows the sign of the difference between path tracking error of using instantaneous and time-averaged flow map for path tracking controller. From Fig. 1c, using time-averaged flow map results in a smaller path tracking error in a small region where $\rho \approx 1$, while using instantaneous flow map leads to smaller path tracking error in other area of the domain. When $\gamma = 0$, there is no tidal component in the domain, thus the instantaneous flow is the same as the time-averaged flow field, and the difference between path tracking error in the two cases is zero.

Then let us consider how the wavelength of spatial variability affects path tracking error. Fig. 2 represents how ω_r affects path tracking error when using instantaneous flow map and time-averaged flow map for path tracking controller. The wavelength is changing from 200 m to 10 km. Glider travels approximately 4 km in one diving-surfacing interval, so the wavelength of spatial variability is one magnitude less than or comparable to the distance glider travels in one lag. From the figure, in case 1, path tracking error decreases as ω_r increases for all $\rho, \gamma \in [0, 1]$, while it stays constant as ω_r increases for all ρ, γ in case 2. Using path tracking controller with the time averaged map results in smaller path tracking error when the spatial variation wavelength is comparable to the distance glider travels in one lag, while using path tracking controller with the instantaneous flow field leads to smaller path tracking error if the wavelength is significantly smaller than the distance glider travels in one interval.

From the above discussion, we have the following conclusions:

1) Value of ρ, γ, ω_r affects the bound of path tracking error if path tracking control is performed with the instantaneous flow field; only γ affects the bound of path tracking error if path tracking control is performed with the time-averaged flow field.

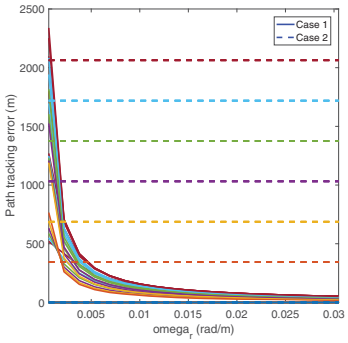

Fig. 2: Numerical simulation showing how the maximum path tracking error in 24 hours changes with respect to ω_r when using instantaneous flow field for flow canceling controller (case 1) and when using time-averaged flow field for flow canceling controller (case 2). In the figure, each of the lines represents how path tracking error evolves with the respect to ω_r with a specific $\rho, \gamma \in [0, 1]$.

2) Performing flow canceling control with time-averaged flow field results in less path tracking error in the case where the strength of the spatially varying flow component is near glider speed, or in the case where the wavelength of spatial variability is relatively large. Otherwise, using the instantaneous flow field for path tracking control will result in less path tracking error.

IV. Simulation Results

The goal for the simulated experiment is to demonstrate the path tracking performance of using both instantaneous and time-averaged flow field for path tracking controller for a simulated glider deployment near Cape Hatteras, NC. Input for path planning and path tracking is given by a HF Radar (High Frequency Radar) product made available by Dana

TABLE I: Identified parameters for the spatial and temporal variation functions of the cross-track flow.

$a_r(m/s)$	$a_t(m/s)$	$\omega_r(rad/m)$	ρ	γ
0.0319	0.1057	2.287×10^{-4}	0.1063	0.3523

Savidge (Skidaway Institute of Oceanography, University of Georgia) and Sara Haines (University of North Carolina at Chapel Hill) that combines long range CODAR and nested high resolution WERA radials, and computes a least squares fit at approximately $5-6$ km resolution. We choose a 36 hour experimental window starting at May 2, 2018 at 12:00 UTC. In the experiment, glider is traveling offshore towards the East, with horizontal through-water speed assigned as 0.3 m/s. In Fig. 3, the starting and goal positions of the simulation are shown as red triangle and red star in the figure. The blue curve represents the time-optimal path planned in the first 25 hours (approximately twice the M_2 period) time averaged flow field using the Level Set Method [16]. The two trajectories are generated by performing path tracking control with instantaneous flow field and the 25 hours time-averaged flow field, respectively. The experiment shows that using the time-averaged flow map results in larger path tracking error.

In order to verify whether the simulation result is consistent with analytical discussion, the cross-track flow speed along the planned path is fitted into the sinusoidal model proposed in Section III. Since the planned path is almost a straight line pointing to the East, the cross-track flow speed is approximated by the N-S flow speed. The temporal average is taken over a 25 hour window, and the residual, or difference between the full signal and the average, describes the temporal variability. Spatial and temporal flow parameters are estimated from the temporal average and the temporal variation data using nonlinear regression [17], and are shown in Table I. The regression fit to spatial variability of the flow field is plotted on Fig. 4. The identified $\omega_r, \omega_t, a_t, a_r$, and also the value of ρ, γ computed from the identified parameters are listed in Table I. ω_r of 2.287×10^{-4} corresponds to a wavelength of approximately 27 km, which is consistent with the scale of spatial variability in both the cross-track flow and simulated glider position in 3. Comparing ρ, γ, ω_r from simulation to Fig. 1c, 2, these parameters fall in the region where using the instantaneous flow field results in less path tracking error than using the time-averaged flow field for path tracking control. Therefore, the simulated experiment results is consistent with the analytical discussion.

From both the numerical simulation and the experiment, considering glider deployment in specific regions, we have the following conclusions:

1) In regions where the instantaneous flow speed does not exceed glider speed, it is more preferred to use instantaneous flow for flow canceling strategy.

2) In regions where the wavelength of spatially varying flow component is relatively small, using the instantaneous flow for flow canceling strategy will result in less path tracking error. For example, for offshore deployment near Gulf Stream, the spatially varying flow component exhibit dramatic change in very short distance. In this scenario, using flow canceling strategy with the instantaneous flow will lead to less path tracking error.

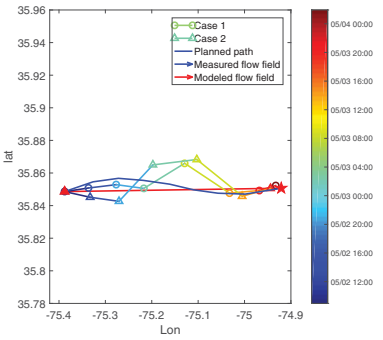

Fig. 3: Simulated glider trajectory of performing path tracking control with instantaneous flow field (case 1) and with time-averaged flow field (case 2). The measured flow field represents time-averaged flow of HF Radar measurement, and the modeled flow field shows the fitted spatial variability of the flow field.

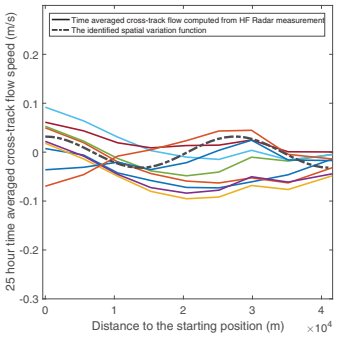

Fig. 4: 25 hours time averaged cross-track flow speed along planned path v.s. distance to the starting position along the planned path. Each of the solid lines is one sampling of cross-track flow at every four hours in the 36 hours experimental window.

3) In regions where the instantaneous flow exceeds glider speed, and the spatially varying flow component does not exhibit periodicity of high frequency, using time-averaged flow map for path tracking control will lead to less path tracking error. For example, for the inshore deployment near Cape Hatteras, the instantaneous flow can be comparable to or exceeds glider speed, while the spatial variability exhibit relatively small change over space. In this case, using time averaged flow map for path tracking will produce less path tracking error.

V. Conclusion

In this work, analytical discussion of path tracking error comparison between performing path tracking control with instantaneous flow field and time-averaged flow field is presented. We showed that in the case where the spatially varying flow of relatively high speed, using the time-averaged flow field for path tracking control results in less path tracking error, while using the instantaneous flow field results in less path tracking error otherwise. Further, we have shown that the scale of spatial variability matters for the choice of flow map input to path tracking controller. Performing path tracking control with time-averaged flow field leads to less path tracking error if the spatial variability is of very low frequency, while using the instantaneous flow field for path tracking control will result in less path tracking error in the case where spatial variability has high frequency. The relative strength of the spatial and temporal variability to vehicle speed can be used to guide the choice of path tracking control scheme. Simulation results are presented to support the analytical results.

Acknowledgment

The research work is supported by ONR grant N00014-16-1-2667, NSF grant OCE-1559475, NOAA grant NA16NOS0120028, and National Natural Science Foundation of China Grant No. 61673370.

References

[1] K. Lynch, I. Schwartz, P. Yang, and R. Freeman, "Decentralized environmental modeling by mobile sensor networks," in *IEEE Transaction of Robotics*, vol. 24, no. 3, 2008, pp. 710–724.

[2] F. Zhang, D. M. Fratantoni, D. A. Paley, J. M. Lund, and N. E. Leonard, "Control of coordinated patterns for ocean sampling," *International Journal of Control*, vol. 80, no. 7, pp. 1186–1199, 2007.

[3] N. E. Leonard, D. A. Paley, R. E. Davis, D. M. Fratantoni, F. Lekien, and F. Zhang, "Coordinated control of an underwater glider fleet in an adaptive ocean sampling field experiment in Monterey Bay," *Journal of Field Robotics*, vol. 27, no. 6, pp. 718–740, 2010.

[4] D. Rudnick, D. Costa, K. Johnson, C. Lee, and M.-L. Timmermans, "ALPS II Autonomous lagrangian platforms and sensors. A report of the ALPS II workshop," Tech. Rep., 2018.

[5] H. Stommel, "The slocum mission," *Oceanography*, vol. 2, pp. 22–25, 1989.

[6] D. C. Webb, P. J. Simonetti, and C. P. Jones, "Slocum: an underwater glider propelled by environmental energy," *Oceanic Engineering, IEEE Journal of*, vol. 26, no. 4, pp. 447–452, 2001.

[7] J. Sherman, R. E. Davis, W. B. Owens, and J. A. Valdes, "The autonomous underwater glider "Spray"," *IEEE Journal of Oceanic Engineering*, vol. 26, no. 4, pp. 437–446, 2001.

[8] C. C. Eriksen, T. J. Osse, R. D. Light, T. Wen, T. W. Lehman, P. L. Sabin, J. W. Ballard, and A. M. Chiodi, "Seaglider: A long-range autonomous underwater vehicle for oceanographic research," *IEEE Journal of Oceanic Engineering*, vol. 26, no. 4, pp. 424–436, 2001.

[9] D. Chang, F. Zhang, and C. R. Edwards, "Real time guidance of underwater gliders assisted by predictive ocean models," *Journal of Atmospheric and Oceanic Technology*, vol. 32, no. 3, pp. 562–578, 2015.

[10] K. Szwaykowska and F. Zhang, "Controlled Lagrangian particle tracking error under biased flow prediction," in *2013 American Control Conference*, Washington, DC, USA, 2013, pp. 2575–2580.

[11] M. Rixen, E. Ferreira-Coelho, and R. Signell, "Surface drift prediction in the Adriatic Sea using hyper-ensemble statistics on atmospheric, ocean and wave models: Uncertainties and probability distribution areas," pp. 86–98, 2008.

[12] M. Hou, S. Liu, F. Zhang, and C. R. Edwards, "A combined path planning and path following method for underwater glider navigation in a strong, dynamic flow field," in *OCEANS'18 Kobe, Japan*, in press.

[13] K. Szwaykowska, "Controlled Lagrangian particle tracking: Analyzing the predicatability of trajectories of autonomous agents in ocean flows," Ph. D. thesis, Georgia Institute of Technology, 2014.

[14] S. Cho and F. Zhang, "An adaptive control law for controlled lagrangian particle tracking," in *Proceedings of the 11th ACM International Conference on Underwater Networks & Systems*, ser. WUWNet '16, 2016, pp. 11:1–11:5.

[15] A. E. Bryson and Y. Ho, *Applied Optimal Control: Optimization, Estimation and Control*. CRC Press, 1975.

[16] J. A. Sethian, *Level Set Methods: Evolving Interfaces in Geometry, Fluid Mechanics, Computer Vison and Material Science*. Cambridge University Press, 1996.

[17] G. A. F. Seber and C. J. Wild, *Nonlinear Regression*. Weiley-Interscience, 1989.